Multi-Scale MHD Simulation Incorporating Pressure Transport Equation for LHD Plasma

Katsuji ICHIGUCHI and Benjamin A. CARRERAS[1)]

National Institute for Fusion Science, Oroshi-cho 322-6, Toki 509-5292, Japan
[1)] *BACV Solutions Inc., 110 Mohawk, Oak Ridge, Tennessee 37831, USA*

(Received: 1 September 2008 / Accepted: 5 October 2008)

A new multi-scale numerical scheme for the nonlinear MHD analysis of heliotron plasmas has been developed as an extension of the original scheme [K.Ichiguchi and B.A.Carreras, Plasma Fus. Res. **3** (2008) S1033]. The time evolution of the dynamics can be studied with this scheme as beta increases. This scheme is based on the iteration of a dynamics calculation utilizing the reduced MHD (RMHD) equations and a calculation of a three-dimensional static equilibrium. The effects of the diffusion of the background pressure and the continuous heating are incorporated in the average pressure equation, which plays a role of a transport equation. This scheme is applied to the inward-shifted Large Helical Device (LHD) plasma to see how the effects influence the self-organization of the plasma.

Keywords: MHD, nonlinear dynamics, multi-scale numerical scheme, interchange mode, heliotron

1. Introduction

To understand consistently the MHD dynamics of the magnetically confined plasma in the increase of beta, it is necessary to examine a continuous evolution of the plasma. In this case, we have to treat the time evolution of the perturbation and the equilibrium simultaneously. However, the perturbation evolves in a short time scale and the equilibrium changes in a long time scale. The difference of the time scale between them is $\sim 10^5$ in general. In the previous work, we developed a numerical scheme to treat this multi-scale problem[1, 2]. The scheme is based on the iteration of the nonlinear evolution of the perturbation dynamics and the update of the static equilibrium. The NORM code[3, 4] is utilized for the dynamics calculations which is based on the RMHD equations, and the VMEC code[5] is used for the equilibrium update which is a three-dimensional equilibrium solver. We applied the scheme to the LHD plasma in the Mercier unstable configuration. It was observed that self-organization of the resistive interchange mode brings local improvement of the Mercier stability[2].

It is a key issue how to treat the time evolution of the background pressure in the multi-scale calculation. In the original scheme[2], we increase the beta by adding a small pressure increment to the average pressure in the equilibrium calculation with the VMEC code. The nonlinear dynamics is calculated with the fixed equilibrium pressure for a short time section. Since the whole time evolution is obtained as a series of the sections, the beta value is increased stepwise inherently. Besides, the diffusion of the background pressure is not taken into account. The background diffusion can affect the local stabilization of the interchange mode through the change of the pressure gradient.

In the present study, we incorporate the effects of the continuous heating and the background pressure diffusion in the multi-scale scheme. For this purpose, we decompose the pressure into the average and the oscillating parts and apply them to the RMHD equation. Since we can regard the average part as the background pressure, we can treat the equation for the average pressure as an equation for the dynamics of the background pressure. The parallel and perpendicular diffusion terms in the equation automatically correspond to the classical diffusion of the background pressure. By adding the heat source term to the equation, we can incorporate the continuous heating effect. There also exists a convection term in the equation. This term indicates anomalous diffusion due to the MHD turbulence. Hence, the equation for the average pressure is regarded as a transport equation for the background pressure, which consists of the classical diffusion, the anomalous diffusion and the heat source. Thus, by utilizing this equation, we can analyze the nonlinear evolution incorporating the effects of the continuous heating and the background diffusion.

We apply this scheme to the nonlinear evolution of the LHD plasma. We observe how the effects of the continuous heating and the background diffusion work on the self-organization of the plasma pressure.

2. Pressure Transport Equation

The present multi-scale scheme is also based on the iteration of the calculations of the nonlinear dynamics and the update of the static equilibrium. The nonlinear dynamics is calculated based on the RMHD equations for stellarators including higher order toroidal corrections[6, 7]. The RMHD equations

author's e-mail: ichiguch@nifs.ac.jp

are the three-field equations for the poloidal flux Ψ, the stream function Φ and the plasma pressure P. In the present scheme, we decompose P differently from Ψ and Φ. The variables of Ψ and Φ are decomposed into the equilibrium and the perturbed parts as

$$\Psi(\rho,\theta,\zeta;t) = \Psi_{eq}(\rho) + \tilde{\Psi}(\rho,\theta,\zeta;t) \tag{1}$$

$$\Phi(\rho,\theta,\zeta;t) = \tilde{\Phi}(\rho,\theta,\zeta;t). \tag{2}$$

On the other hand, P is decomposed into the average and the oscillating parts as

$$P(\rho,\theta,\zeta;t) = \langle P\rangle(\rho;t) + \widehat{P}(\rho,\theta,\zeta;t). \tag{3}$$

Here we employ the flux coordinates (ρ,θ,ζ), where ρ denotes the square root of the normalized toroidal magnetic flux, and θ and ζ are the poloidal and the toroidal angles, respectively. The subscript 'eq' and the tilde indicate the equilibrium and the perturbed quantities, respectively, in Eqs.(1) and (2). The angle bracket and the hat indicate the average and the oscillating parts, respectively, in Eq.(3).

By substituting these decompositions into the normalized RMHD equations, we obtain

$$\frac{\partial\tilde{\Psi}}{\partial t} = -\nabla_\parallel\tilde{\Phi} + \frac{1}{S}\tilde{J}_\zeta, \tag{4}$$

$$\frac{\partial\tilde{U}}{\partial t} = -[\tilde{U},\tilde{\Phi}] - \nabla_\parallel\tilde{J}_\zeta - [\tilde{\Psi},J_{\zeta eq}] + \frac{1}{2\epsilon^2}[\Omega_{eq},\widehat{P}] + \nu\left(\frac{R}{R_0}\right)^2\nabla_\perp^2\tilde{U}, \tag{5}$$

$$\frac{\partial\langle P\rangle}{\partial t} = -\langle[\widehat{P},\tilde{\Phi}]\rangle + \kappa_{\perp 0}\langle\Delta_*\langle P\rangle\rangle + \kappa_{\parallel 0}\langle\nabla_\parallel^{\dagger 2}\langle P\rangle\rangle + Q, \tag{6}$$

$$\frac{\partial\widehat{P}}{\partial t} = -\widehat{[P,\tilde{\Phi}]} + \kappa_\perp\widehat{\Delta_* P} + \kappa_\parallel\widehat{\nabla_\parallel^{\dagger 2}P}. \tag{7}$$

Here $[y,z]$ denotes the Poisson bracket which is defined as

$$[y,z] = \frac{g}{\rho}\left(\frac{\partial y}{\partial\rho}\frac{\partial z}{\partial\theta} - \frac{\partial y}{\partial\theta}\frac{\partial z}{\partial\rho}\right). \tag{8}$$

The diffusion operators Δ_* and $\nabla_\parallel^{\dagger 2}$ are also defined as

$$\Delta_* f = \left(\frac{R}{R_0}\right)^2\nabla_\perp\cdot\left(\frac{R_0}{R}\right)^2\nabla_\perp f \tag{9}$$

and

$$\nabla_\parallel^{\dagger 2} f = \nabla_\parallel\left[\left(\frac{R_0}{R}\right)^2\nabla_\parallel f\right], \tag{10}$$

respectively, where R/R_0 denotes the normalized major radius. The perpendicular and the parallel differential operators are given by

$$\nabla_\perp f = \nabla f - \nabla\zeta\frac{\partial f}{\partial\zeta} \tag{11}$$

and

$$\nabla_\parallel f = g\frac{\partial f}{\partial\zeta} + [\Psi,f], \tag{12}$$

respectively, where g is a factor corresponding to the diamagnetic effect. The variables of U and J_ζ are the vorticity and the toroidal current density which are given by $U = (R/R_0)^2\nabla_\perp^2\Phi$ and $J_\zeta = \Delta_*\Psi$, respectively. These variables are decomposed as in the cases for Φ and Ψ. The equilibrium quantity $\nabla\Omega_{eq}$ gives average field line curvature. The factors ϵ, S, ν, $\kappa_\perp$ and $\kappa_\parallel$ are the plasma aspect ratio, the magnetic Reynolds number, the viscosity coefficient, the perpendicular heat conductivity and the parallel heat conductivity, respectively. The heat source term Q is added in Eq.(6).

In this formulation, we treat $\langle P\rangle$ as the background equilibrium pressure. Hence, Eq.(6) can be regarded as a transport equation for the background pressure. The equation consists of the convection term, the perpendicular and the parallel diffusion terms and the heat source term. These terms have the effects of the anomalous diffusion due to the nonlinear turbulence, the classical heat conductivity and the continuous heating for the background pressure, respectively. By using the equation, we can follow the dynamics of the background pressure incorporating the continuous heating and the background diffusion.

The equations (4)-(7) are solved by utilizing the NORM code. Details of the NORM code are explained in Ref.[3].

3. Multi-Scale Numerical Scheme

In the present scheme, we consider a short time interval as a calculation unit. The whole time evolution is obtained as a series of the results of the intervals. The numerical procedure for an interval of $t_i \le t \le t_{i+1}$ is explained here.

Since the NORM calculation of the previous interval finishes at $t = t_i$, we have the average pressure $\langle P\rangle_i$ at this time. The subscript 'i' means the value at $t = t_i$. Here we use $\langle P\rangle_i$ as the equilibrium pressure at $t = t_i$,

$$P_{eq,i} = \langle P\rangle_i. \tag{13}$$

Then, we calculate the equilibrium quantities $E_{eq,i}$ for $P_{eq,i}$ by using the VMEC code. We also calculate the equilibrium quantities $E^G_{eq,i+1}$ at $t = t_{i+1}$ for $P^G_{eq,i+1}$ which is given by

$$P^G_{eq,i+1} = P_{eq,i} + \Delta P(\rho). \tag{14}$$

Here ΔP denotes the increment of the pressure that increases beta. Then, we interpolate the equilibrium quantities to obtain the values at every time step of the dynamics calculation with the NORM code. If the

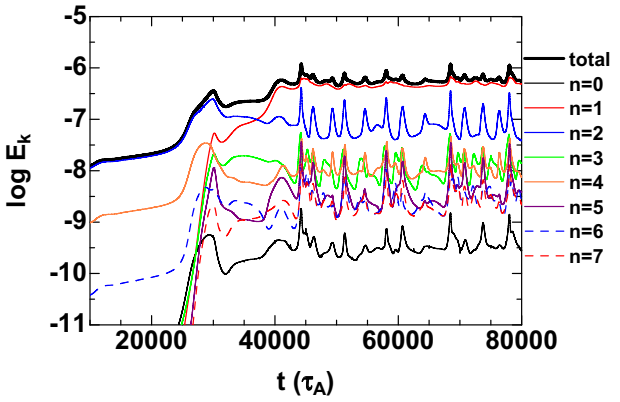

Fig. 1 Time evolution of kinetic energy.

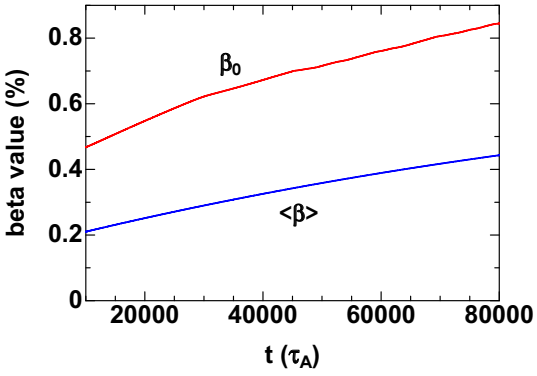

Fig. 2 Time evolution of beta values.

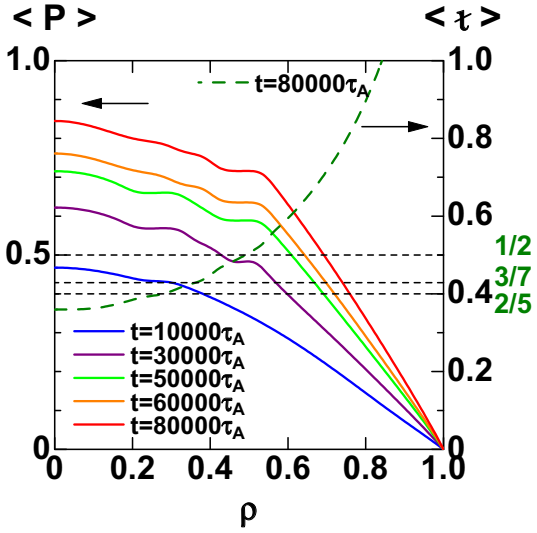

Fig. 3 Profiles of average pressure at $t = 10,000\tau_A$, $30,000\tau_A$, $50,000\tau_A$, $60,000\tau_A$ and $80,000\tau_A$. Profile of rotational transform at $t = 80,000\tau_A$ is also plotted.

number of the time step is L for $t_i \le t \le t_{i+1}$, we can obtain the interpolated equilibrium quantities at j-th step as

$$E^G_{eq,ij} = E_{eq,i} + \frac{j}{L}(E^G_{eq,i+1} - E_{eq,i}) \tag{15}$$

except $J^G_{\zeta eq,ij}$. The value of $J^G_{\zeta eq,ij}$ is determined so that the equilibrium equation

$$-[\Psi^G_{eq,ij}, J^G_{\zeta eq,ij}] + [\Omega^G_{eq,ij}, \langle P\rangle_{ij}] = 0 \tag{16}$$

is satisfied. The heat source term in Eq.(6) is determined so as to be consistent with the pressure increment as

$$Q = \frac{\Delta P}{L\Delta t}, \tag{17}$$

where Δt denotes the time step in the NORM calculation. Thus, the dynamics for the interval is calculated with the equilibrium quantities of $E^G_{eq,ij}$ by using the NORM code. We obtain $\langle P\rangle_{i+1}$ at the end of the interval, which is used for the calculation of the next interval.

In this procedure, the continuity of the equilibrium pressure is not guaranteed because $\langle P\rangle_{i+1}$ does not necessarily equal to $P^G_{eq,i+1}$. To reduce the difference and keep the continuity we employ a corrector calculation. Once we finish the NORM calculation at $t = t_{i+1}$, we set

$$P^{G2}_{eq,i+1} = \langle P\rangle_{i+1}. \tag{18}$$

Then, we calculate the equilibrium quantities and follow the nonlinear dynamics again using $P^{G2}_{eq,i+1}$ instead of $P^G_{eq,i+1}$.

4. Application to LHD Plasma

We apply the scheme to the LHD plasma in the configuration with the vacuum magnetic axis located at $R_{ax} = 3.6$m. We assume the dissipation parameters of $S = 10^6$, $\nu = 1.5 \times 10^{-4}$, $\kappa_\perp = \kappa_{\perp 0} = 1.5 \times 10^{-6}$ and $\kappa_\parallel = \kappa_{\parallel 0} = 1.5 \times 10^{-2}$. We examine the time evolution for $0.210\% \le \langle\beta\rangle \le 0.443\%$. The length of one time interval is $2500\tau_A$, where τ_A is Alfvén time. We increase the beta value by $\Delta\langle\beta\rangle = 0.00832\%$ every time interval. In the equilibrium calculation with the VMEC code, we use the free boundary condition and the no net-current condition.

To obtain the initial state, we start from the equilibrium for

$$P_{eq} = P_0(1-\rho^2)(1-\rho^8) \tag{19}$$

at $\langle\beta\rangle = 0.210\%$. The core region of $\rho \le 0.53$ of this equilibrium is Mercier unstable. Therefore, the interchange mode linearly grows. We follow the nonlinear evolution of the mode for this equilibrium using the present scheme with $\Delta P = 0$ and obtain a saturation at $t = 10,000\tau_A$. In this case, the $(m, n) = (5, 2)$ mode dominantly grows and saturates. We employ the saturated state as the initial state of the beta-increasing calculation and set $t = 10,000\tau_A$ as the initial time.

Figure 1 shows the time evolution of the kinetic energy. In the VMEC calculation, we use the same

profile of the equilibrium pressure for the pressure increment ΔP. In this case, the beta value increases as shown in Fig.2. In this scheme, as explained in Sec.3, the continuity of the equilibrium quantities is not necessarily guaranteed when the equilibrium is updated by using the VMEC code. Nevertheless, not only the total energy but also each component vary smoothly as the beta increases. This result indicates that the scheme treats the continuous evolution of the whole system very well.

As in the case of the initial state calculation, the $(5,2)$ interchange mode is dominant for $t \lesssim 20,000\tau_A$. This mode generates a local flat region in the average pressure profile in the vicinity of the resonant surface with $\iota = 2/5$ as shown in Fig.3. A pentagon-like structure is formed in the total pressure profile as shown in Fig.4(a). Since the local flattening of the pressure profile steepens the gradient of the both sides of the flat region. Therefore, the $(4,2)$ mode is excited at the surface with $\iota = 1/2$ at $t \simeq 25,000\tau_A$, and the $(2,1)$ mode becomes dominant $t \simeq 40,000\tau_A$. These modes generate another local flat structure in the average pressure profile for $30,000\tau_A \lesssim t \lesssim 50,000\tau_A$.

For $t \gtrsim 50,000\tau_A$ the total kinetic energy is almost constant and small tips frequently appear. The tips are attributed to the excitation of the $(5,2)$ mode. In this region, the $(2,1)$ mode is continuously dominant, however, the kinetic energy of the mode varies weakly. The enhancement time of the $(2,1)$ mode does not always coincide with the excitation time of the $(5,2)$ mode. This time difference is due to the fact that the $(5,2)$ and $(2,1)$ modes interact each other through the deformation of the average pressure profile. The excitation of $(2,1)$ mode enhances the pressure gradient at the region with $\iota = 2/5$. Then, the $(5,2)$ mode is excited. On the other hand, the excitation of $(5,2)$ mode enhances of the pressure gradient at the region with $\iota = 1/2$, which leads to the excitation of the $(2,1)$ mode.

Since the local flat structure is already generated at both $\iota = 2/5$ and $\iota = 1/2$ before the interaction, the amplitude of the modes does not reach a high level. On the other hand, both effects of the continuous heating and the background diffusion continuously enhances the gradient of the average pressure. Therefore, the effects always give a driving force to the modes, particularly in their saturation phase. As a result, small scale excitation and saturation are repeated frequently.

As shown in Fig.3, the $\langle P \rangle$ profile shows a global gradient in the core region for $t \geq 60,000\tau_A$, which is different from the initial gradient. On the other hand, the amplitude of the oscillating parts of the pressure is reduced at $t = 80,000\tau_A$ compared with that at $t = 30,000\tau_A$ as shown in Fig.4(b) and (c). These

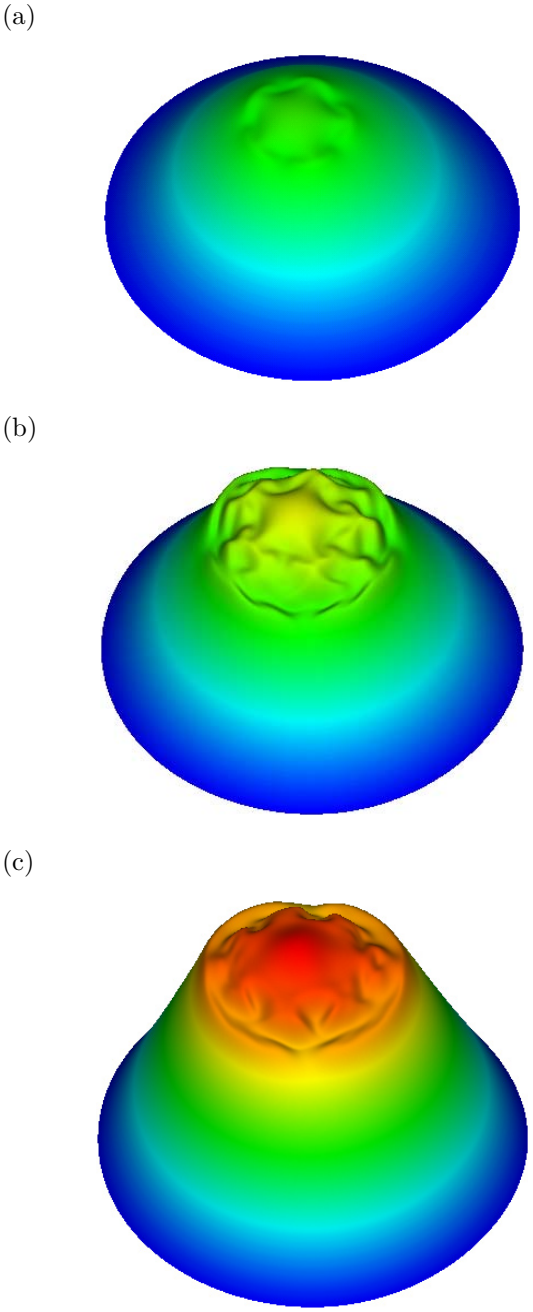

Fig. 4 Bird's eye view of total pressure profile at (a) $t = 10,000\tau_A$, (b) $t = 30,000\tau_A$ and (c) $t = 80,000\tau_A$.

tendencies indicate that the average pressure is self-organized so as to approach a marginally stable state through the repetition of the mode excitation and saturation.

5. Concluding Remarks

In order to analyze the nonlinear MHD dynamics in the beta increase phase, we have developed a multi-scale MHD simulation scheme incorporating a pressure transport equation by extending the original multi-scale scheme. In the present scheme, the equation for the average pressure in the RMHD equation

expresses the dynamics of the background pressure. The terms of the heat source and the background pressure diffusion are included in this equation. Therefore, this equation plays a role of a transport equation.

The scheme is applied to the low-beta inward-shifted LHD plasma. Self-organization of the pressure profile is obtained as a result of the frequent interaction of the weak interchange modes resonant at the different regions. The continuous heating and the background diffusion are crucial for the frequent weak activity. In the self-organization, the reconstruction of a global pressure gradient and the reduction of the mode amplitude are seen as beta increases. This tendency indicates a stable path to a high beta regime, which has been achieved in the experiments[8].

The self-organized profile of the average pressure is similar to that obtained with the original scheme[2]. However, the precise structure is different. In the original scheme, the beta value is increased stepwise and the nonlinear dynamics is calculated for fixed equilibria in short time sections. In this case, there exists a longer time for the modes to saturate than in the present scheme. Therefore, the self-organized pressure profile tends to have a uniform structure in the poloidal direction. On the other hand, in the present scheme, the effects of the continuous heating and the background diffusion continuously enhances the pressure gradient. The interchange mode is easily excited even in the local flat region of the average pressure profile. Then the modes in the different regions can be excited alternately through the local deformation of the average pressure profile. Thus, as shown in Fig.4(c), a poloidal structure corresponding to the resonant mode tends to remain in the pressure profile when the plasma is close to the marginally stable state.

Acknowledgments

This work is supported by NIFS cooperation program NIFS08KNXN129 and the Grant-in-Aid for Scientific Research (C) 17560736 of the Japan Society for the Promotion of Science.

References

[1] K. Ichiguchi B. A. Carreras, J. Plasma Phys. **72** 1117-1121, (2006).
[2] K. Ichiguchi B. A. Carreras, Plasma Fus. Res. **3** S1033, (2008).
[3] K. Ichiguchi, et al., Nucl. Fusion **43**, 1101-1109 (2003).
[4] K. Ichiguchi, et al., Fusion Science and Technology **46**, 34-43 (2004).
[5] Hirshman, S. P., et al., Comput. Phys. Commun. **43**, 143-155 (1986).
[6] Y. Nakamura, et al., J. Comp. Phys. **128**, 43-57 (1996).
[7] K. Ichiguchi, et al., Nucl. Fusion **33**, 481-492 (1993).
[8] Y. Takeiri, et al., Proc. of Joint Conf. 17th Int. Toki Conf. 16th Int. Stellarator/Heliotron Workshop 2007, Oct. 15-19, 2007, Toki, R-01 (2007).